Acta Materialia 168 (2019) 353–361

Contents lists available at ScienceDirect

Acta Materialia

journal homepage: www.elsevier.com/locate/actamat

Full length article

Role of local stresses on co-zone twin-twin junction formation in HCP magnesium

M. Arul Kumar [a, *], M. Gong [a, b], I.J. Beyerlein [c], J. Wang [b], C.N. Tomé [a]

[a] Materials Science and Technology Division, Los Alamos National Laboratory, Los Alamos, NM, 87545, USA
[b] Department of Mechanical and Materials Science Engineering, University of Nebraska, Lincoln, NE, 68588, USA
[c] Department of Mechanical Engineering, Materials Department, University of California at Santa Barbara, Santa Barbara, CA, 93106, USA

ARTICLE INFO

Article history:
Received 28 September 2018
Received in revised form
21 February 2019
Accepted 22 February 2019
Available online 26 February 2019

Keywords:
Twin-twin junction
Local stresses
Crystal plasticity
Molecular dynamics
Magnesium

ABSTRACT

Twin-twin interactions control the formation of twin-twin junctions (TTJ) in hexagonal metals when multiple twin variants are activated in a grain. In this work, we employ a combination of two computational techniques, a 3D full-field crystal plasticity model (CP) and large-scale molecular dynamics (MD), to study the TTJ formation associated with two non-parallel $\{10\bar{1}2\}$ twins in Mg. The local intra-granular stresses generated by discrete twins are computed using a spatially resolved CP model. Atomic-scale knowledge regarding formation processes and local stresses is revealed by MD. The combined analyses suggest that the twin junction forms by the migration of the boundaries of both, the impinging and impinged twin, taking place in the immediate vicinity of the contact point. It is further shown that local stress fields that are generated after initial contact promote thickening of the impinging twin, and may facilitate nucleation of a new twin on the opposite boundary of the recipient twin. Calculations of the strain energies suggest that formation of the co-zone twin-twin junction is energetically favorable but detwinning of the TTJ upon load reversal or under cyclic loading is not.

Published by Elsevier Ltd on behalf of Acta Materialia Inc.

1. Introduction

Lightweight magnesium (Mg) and its alloys are being widely used in structural components [1–4]. Thus, motivates the need to understand their deformation behavior, particularly when they are strained beyond their elastic limit. Important in the plastic deformation of Mg and its alloys are two mechanisms: the motion of dislocations, and the formation and propagation of deformation twins. The stresses required to activate and propagate these mechanisms translate to their yield strength, peak strength, and ductility [5–7]. Deformation twins are sub granular domains that impart shear on the surrounding crystal and bear a distinctly different crystallographic orientation. They typically grow to span the grain cross-section [5,8–12], their influence on plastic response is less well understood than the one of slip. Twin size, number, and configuration, can have a profound effect on plastic anisotropy, yield strength, flow stress, hysteresis in cyclic loading, and strain hardening. The shear they impose generates local stress fields that can affect recrystallization, cracking, void formation, and coalescence to failure [13–21].

For these reasons, many studies have sought to understand the development of microscopic details of twin lamellae within grains, such as the variables that dictate their size, shape, arrangement, variant selection, and their transmissibility across grain boundaries [8–10,12,22–29]. The common picture of a twinned granular microstructure consists of grains containing many parallel twins of the same variant (lattice orientation) [8,12,27,30]. In many alloys, however, twinning can be sufficiently profuse that multiple, non-parallel twin variants can form within a grain, forming a 3D twin network connected by twin-twin junctions (TTJs) [10,31–40]. Activation of non-parallel twin variants is found in materials with heterogeneous grain microstructure, in grains favorably oriented with respect to the applied stress, and in the case of complex loading conditions [20,21,31,37]. In particular, recent works have demonstrated that twin junctions can play a distinctive role compared to isolated twins in what concerns interaction with glide dislocations, further twinning, local strain hardening, and void formation and fracture [10,20,31,37,38,41,42]. For example, El-Kadiri et al. [31] showed that in Mg twins forming junctions are less likely to thicken than isolated twins. As a result, twin propagation entails forming new twin lamellae. To demonstrate that, they closely examined two

* Corresponding author.
E-mail address: marulkr@lanl.gov (M. Arul Kumar).

https://doi.org/10.1016/j.actamat.2019.02.037
1359-6454/Published by Elsevier Ltd on behalf of Acta Materialia Inc.

grains with roughly the same Schmid factor, one showing a single twin variant and the other two intersecting twin variants. Upon further loading, the pre-existing twins grew in the former grain, but not in the latter. At the same time, in the twin intersecting grain new twins formed, suggesting that the presence of TTJs favors the nucleation of new twins and hinders the growth of existing twins. A statistical study by Juan et al. [10] on Zirconium (Zr) demonstrated a similar impeding effect of twin junctions on twin thickening. Jiang et al. [42] and Yu et al. [37] reported that an increase in the number of twin junctions increases the strain-hardening rate in AZ31 Mg alloy and pure Mg, respectively.

Most of the available works aiming to understand the formation and evolution of TTJs have been experimental and only provide partial information [35,37–39]. In efforts to provide understanding concerning the micromechanics of junction formation, recent work of Xu et al. [39] calculated the local stresses associated with TTJs using continuum mechanics Finite Element modeling, which approximates the material as a linear elastic solid. The results account for the formation of the preferred configuration of twin junctions. Note, however, that plastic relaxation greatly affects the calculation of the local stress fields and further twinning [25,27,43–46], and a full-field elastic-plastic analysis is required for understanding local stress states associated with the formation and evolution of TTJs.

In this work, we study local stress states associated with the formation and evolution of TTJs by employing a crystal plasticity Fast Fourier Transform approach developed to model deformation twinning in HCP metals [27,45]. The advantage of this approach is that the spatially resolved stress fields can be calculated based on the local anisotropic elasticity and plasticity of the crystal. It treats much larger length scales than atomic scale simulations, and therefore examines stress fields of different possible variants and configurations of twins. However, local atomic processes, particularly those responsible for the migration of two interacting twin boundaries, cannot be explicitly modeled. For determining the atomic level characteristics of boundary migration suggested by the calculated stress fields, we employ molecular dynamics simulations of the same twin junction. The combined analyses show that the local stress fields promote twin-twin junction formation, and that the process is energetically favorable. It also suggests that under a load reversal, migrating the twins apart becomes increasingly unfavorable the closer the twins become, and breaking the twin-twin junction after it has formed is unfeasible. Most interestingly, the calculations indicate that twins do not transmit across one another but that the twin impinging on one boundary, may re-nucleate on the opposite boundary of the impinged twin.

2. Numerical simulation

2.1. Crystallography of twin-twin junction

Twin-twin junctions can be broadly classified into three types based on the relative orientation of the participating variants. In an HCP crystal, every twin type has six different variants. The first junction type (type-I) is called a co-zone junction where two twins share the same zone axes. The second (type-II) and third (type–III) are called non-co-zone junctions. The minimum angles between the zone axes of the twins are $2\pi/3$ and $\pi/3$ for type II and type III junctions, respectively. Both co-zone and non-co-zone types junctions have been observed in many structural HCP metals, like Mg and Zr [10,31,35,37]. Fig. 1(a) shows examples of experimentally observed co-zone junctions in single crystal Mg compressed along $[10\bar{1}0]$ direction [37].

In this work, we focus on the most commonly observed co-zone twin junction in HCP Mg. Without loss of generality, we treat the case of two twin variants making a co-zone junction with the following crystallography: T1 $((10\bar{1}2)[\bar{1}011])$ and T4 $((\bar{1}012)[10\bar{1}1])$, and as shared zone axis $[\bar{1}2\bar{1}0]$, see Fig. 1(b). With this crystallography the problem becomes a two-dimensional one with the zone axis as the plane normal.

2.2. Full-field fast fourier transform model

To calculate the local stresses around twin-twin junctions, we employ a version of a full-field, elasto-visco-plastic Fast Fourier Transform (EVP-FFT) model that has been created to treat discrete twin lamella [27,45]. The original FFT formulation was developed to study the local and effective mechanical response of composite materials [47,48]. Later, Lebensohn [49] adapted it for polycrystalline materials to study the effective and local responses associated with the heterogeneity in the spatial distribution of crystallography and directional dependence of mechanical properties. This basic FFT formulation has been extended to different deformation regimes like elasticity [50], incompressible visco-plasticity [49,51], dilatational visco-plasticity [52], infinitesimal elasto-visco-plasticity [53,54] and finite elasto-visco-plasticity [55]. The current EVP-FFT version used here incorporates the twin transformation strain in regions predefined with a twin orientation. It has been successfully applied to study neighboring grain and grain size effect on twin growth, parallel twin formation and twin transmission cross grain boundaries [25–27,43,44].

The twin FFT model builds upon an infinitesimal elasto-visco-plastic formulation. Within this framework, the deformation twin is a domain that undergoes a shear transformation. Taken together, the constitutive behavior for an elasto-visco-plastic material under an infinitesimal strain approximation including the shear transformation is given by

$$\boldsymbol{\sigma}(x) = \boldsymbol{C}(x) : \boldsymbol{\varepsilon}^{e}(x) = \boldsymbol{C}(x) : \left(\boldsymbol{\varepsilon}(x) - \boldsymbol{\varepsilon}^{p}(x) - \boldsymbol{\varepsilon}^{tr}(x)\right) \tag{1}$$

In the above expression, $\boldsymbol{\sigma}(x)$ is the Cauchy stress tensor, $\mathbf{C}(x)$ is the elastic stiffness tensor, $\boldsymbol{\varepsilon}(x)$, $\boldsymbol{\varepsilon}^{e}(x)$, and $\boldsymbol{\varepsilon}^{p}(x)$ are the total, elastic and plastic strain tensors, and $\boldsymbol{\varepsilon}^{tr}$ is the transformation strain. The local stress field at a material point x is solved using an implicit time discretization of the form:

$$\boldsymbol{\sigma}^{t+\Delta t}(x) = \mathbf{C}(x) : \left(\boldsymbol{\varepsilon}^{t+\Delta t}(x) - \boldsymbol{\varepsilon}^{p,t}(x) - \dot{\boldsymbol{\varepsilon}}^{\mathrm{p,t+\Delta t}}(x)\Delta t - \boldsymbol{\varepsilon}^{\mathrm{tr,\ t}}(x) - \Delta\boldsymbol{\varepsilon}^{\mathrm{tr,t+\Delta t}}(x)\right) \tag{2}$$

Within the twin domain, twin transformation strain is imposed. To build-up the twinning transformation, successive shear increments are imposed within the twin domain using the following strain increments:

$$\Delta\boldsymbol{\varepsilon}^{tr}(x) = \mathbf{m}^{tw}(x)\Delta\gamma^{tw}(x) \tag{3}$$

For material points outside the twin domains, $\Delta\varepsilon^{tr}(x)$ is zero. The tensor $\boldsymbol{m}^{tw} = \frac{1}{2}(\boldsymbol{b}^{tw} \otimes \boldsymbol{n}^{tw} + \boldsymbol{n}^{tw} \otimes \boldsymbol{b}^{tw})$ is the Schmid tensor associated with the twin system, where $\mathbf{b}^{\mathrm{tw}}$ and $\mathbf{n}^{\mathrm{tw}}$ are unit vectors along the twinning direction and the twin plane normal, respectively. The number of increments $\mathrm{N}^{\mathrm{twincr}}$ needed to reach the characteristic-twinning shear, s^{tw} is simply:

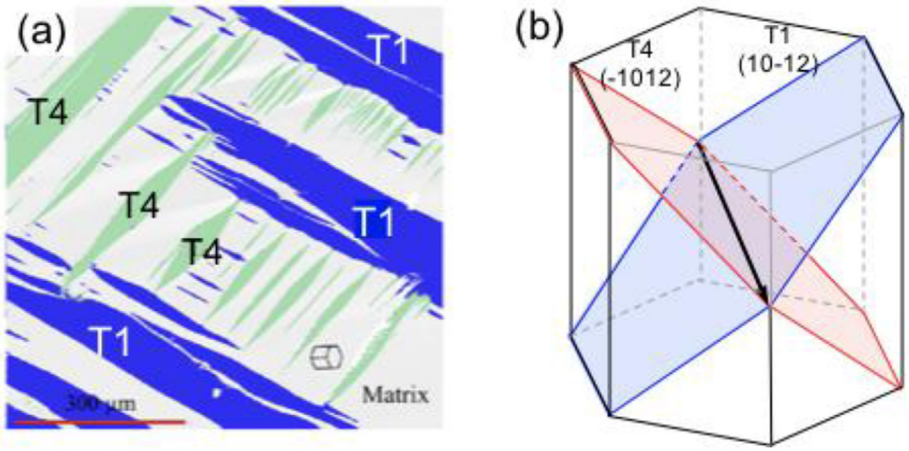

Fig. 1. Experimentally observed twin-twin junctions in single crystal magnesium compressed along $[10\bar{1}0]$ [37]. (b) Schematic representation of the co-zone twin-twin junction considered here, formed by tensile twin variants T1 and T4 sharing the same zone axis.

$$\Delta\gamma^{tw}(x) = \frac{s^{tw}}{N^{twincr}} \tag{4}$$

In the following calculations, we set the time increment Δt and N^{twincr} sufficiently low and high, respectively, to ensure convergence.

2.3. FFT simulation details

In this work we study the role and characteristics of the local stresses and associated energetics on twin-twin junction formation in order to understand the process leading to twin junction. To simplify the analysis, we consider this process within a single grain and effects from neighboring grains are not taken into account.

Fig. 2 shows a schematic representation of the simulation setup. This setup consists of one orientation (grain) finely discretized, which will contain the twins, surrounded by a buffer layer. The unit cell is assumed to be periodic in all three directions and discretized into 3 × 750 x 750 voxels with a buffer layer 25 voxels thick, which is sufficient for making the spatially resolved stress distribution in the cell interior insensitive to how the boundary conditions are applied. Twins are introduced in the center of the unit cell, away from the buffer layer. Each voxel of the buffer layer is assigned a randomly generated crystal orientation. The simulation results that we present here are not affected by the specific thickness and crystal orientation of the buffer layer.

For the following calculations, we select the crystallographic orientation of the grain to be (0°, 0°, 0°), in the Bunge convention, which corresponds to alignment of the $[10\bar{1}0]$ and [0001] axes parallel to Y and Z directions, respectively. The unit cell is subjected to compression along the Y-direction, and thus gives high Schmid factor (~0.5) for both twin variants T1 and T4.

For this combination of grain orientations and loading conditions, the twin plane normal and twin shear directions of both twin variants lie in the Y-Z plane. There is no out-of-plane twin shear in X−Y and X-Z planes. The twin domain in the simulation is assumed to have two parallel interfaces corresponding to the twin plane of each variant. The inclination of the twinning plane with respect to the compression axis is ±43.1°. The twin thickness is spanned by nine voxels, which corresponds to a total twin volume fraction of ~0.95% in the model grain. Initially, the separation between T1 and T4 is *s*, T1 is the impinged twin and T4 the impinging twin. To capture the different stages in junction formation, a series of simulations with different spacings *s* between twins T1 and T4 is performed (see Fig. 2).

To calculate the stress state at each stage it is important to achieve equilibrium for each configuration. For a given configuration of T1 and T4, we perform the following sequence of steps. First the entire unit cell is compressed along the Y-direction under a constant applied strain state to 0.001 strain (compressive stress in Y-direction is ~40 MPa). This imposed strain induces a positive

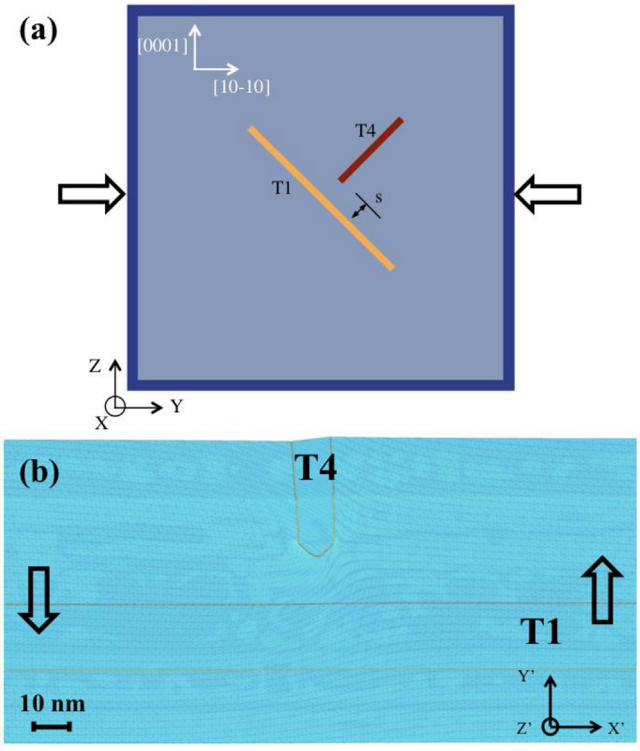

Fig. 2. (a) Schematic representation of the simulation unit cell with two tensile twin variants (T1 and T4). The spacing between twins T1 and T4 is characterized by spacing parameter, *s*; and different *s* values are considered for numerical simulations. The orientation of the parent grain is assumed as (0°, 0°, 0°), i.e., c-axis is parallel to Z-direction, and so the crystal is subjected to in-plane compression. (b) Relaxed MD model prior to twin-twin interaction simulations. Simple shear favoring both T1 and T4 twinning is then applied to this model.

resolved shear stress (RSS) of ~20 MPa on both twin variants. Such value is of the order of the critical resolved shear stress (CRSS) for $\{10\bar{1}2\}$ twin in Mg [56]. Second, twin T1 is introduced, by reorienting the crystal on those voxels pre-selected for the twin domain, and enforcing in this set the twin transformation shear in several increments. In this work, twinning shear (=13% for Mg) is accommodated in 2000 steps. During these steps, the externally imposed strain is fixed. Under this boundary condition, stresses relax after T1 twin transformation, affecting the region where the twin T4 will be introduced, and reducing the RSS on the twin plane T4. Accordingly, before introducing T4, the externally applied compression is increased such that the RSS in the domain of twin T4 becomes slightly greater than the CRSS. Once this state is achieved, the T4 twin is introduced using the same two steps described above for the T1 twin.

At all stages in the simulation, the deformation is accommodated elastically and plastically. The constitutive law material parameters used in simulations are the elastic moduli tensor, the plastic slip modes, and the CRSS values for activating them. For pure Mg, the elastic constants at room temperature used are: $C_{11} = 58.58$, $C_{12} = 25.02$, $C_{13} = 20.79$, $C_{33} = 61.11$ and $C_{44} = 16.58$ GPa [57,58]. Plasticity is accommodated by three slip modes: basal <a>, prismatic <a> and pyramidal ⟨c+a⟩ slip and the corresponding CRSS values are: 3.3, 35.7 and 86.2 MPa, respectively [56]. In these calculations, we expect that work hardening and lattice rotations will be negligible since the calculations involve only a few percent macroscopic strain. Therefore, a constant, non-evolving CRSS value for slip on each slip system will be employed in the calculations here. However, should larger macroscopic strains be desired, hardening effects could easily be considered in this model framework.

2.4. Atomistic simulation details

To reveal the processes underlying junction formation at the atomic scale, we carried out Molecular Dynamics (MD) simulations using an in-house code. The MD model was designed to simulate the interaction of T1 and T4 just prior to and after their contact. The MD calculations employ the EAM empirical interatomic potential for Mg, described in Ref. [59].

The simulation model has dimensions $480 \times 120 \times 1.6$ nm in the x'-, y'- and z'-direction, and periodic boundary conditions are adopted in the z'-direction. The parent crystal containing T1 and T4 adopts the following coordinates: the x'-axis is along $[10\bar{1}1]$ direction, the y'-axis is normal to $(\bar{1}012)$ plane and the z'-axis is along $[1\bar{2}10]$ direction. We begin by introducing T1 in this crystal according to its specific twin/matrix orientation relationship. The T1 lamella is 25.5 nm thick in the y-direction and crosses through the model crystal in the x'- and z'-direction. With T1 in the crystal, the model becomes a sandwiched structure without internal stresses because the upper matrix shifts relative to the lower part of the model due to the net shear associated with T1. Next, T4 is created in the upper matrix by introducing two sets of 20 twinning disconnections associated with T4 (20 on a Basal/Prismatic (BP) plane and 20 on a Prismatic/Basal (PB) plane). The Burgers vector is equal to $(0.003, -0.049, 0)$ nm in the current coordinate system [60]. According to the shear-shuffle mechanism [32,61], the introduction of twinning dislocations (TDs) into the model is first accomplished through the application of the anisotropic Barnett-Lothe solutions for the displacement field of dislocations [62]. This process is performed while fixing a 1 nm wide layer on the surfaces of the cell perpendicular to the x'- and y'-directions in order to preserve the displacement fields associated with T4 twinning. After shearing the crystal associated with the gliding of TDs, atoms in the sheared region are displaced according to the corresponding shuffle vectors [33]. When introduced in this way, the thickness of T4 is 15.1 nm and the twin tip is 18.5 nm away from T1. Energy minimization is then performed with a damped dynamic minimizer for 40 picoseconds to relax the model into near-equilibrium state. During minimization, the velocity v_i ($i = 1, 2, 3$) is set to zero when the dot product of velocity and acceleration is negative.

In the relaxed model shown in Fig. 2(b), T1 is bounded by two flat CTBs while T4 is a blunt twin tip bounded by CTBs, BP and PB facets. The relaxed model is then loaded at 50 K with an applied T4-TRSS of 500 MPa to simulate the interaction processes of twins T1 and T4. The shear stress is achieved by applying a homogeneous deformation gradient to all atoms in the cell, with one non-zero shear component $\mathbf{F_{21}}$. The induced shear stress favors propagation of both, T4 and T1. During loading, position and atomic stress of atoms are output for configurations at all deformation stages.

3. Results and discussion

3.1. Prior to twin-twin contact ($s > 0$)

Calculations are performed to study the stress fields that develop around two co-zone twins as they approach each other prior to contact. The two twins, one T1 and the other T4, have equal thickness t and T4, the impinging twin, approaches T1, the impinged twin. Fig. 3 shows results for the specific case in which the tip of T4 is at a distance twice the twin thickness t from T1. As a way of inferring the forces driving twin migration we analyze the twin resolved shear stress field (TRSS) along the twinning direction of twin variants T1 and T4. This resolved shear could drive glide of twinning dislocations on a coherent twin boundary as well as the climb of disconnections on basal-prism (BP) facets, two mechanisms for twin boundary migration [61,63,64]. An advantage of our calculations is that the full stress and strain tensors can be calculated, and thus all stress components acting on the twin interface can be determined.

Prior to contact, two possible events can enable junction formation: migration of the T1 boundary, the impacted twin, and propagation of T4, the impinging twin. Our previous analysis of the stress field surrounding isolated twins indicates that ahead of the twin tip the TRSS is positive and favorable to propagation, while in

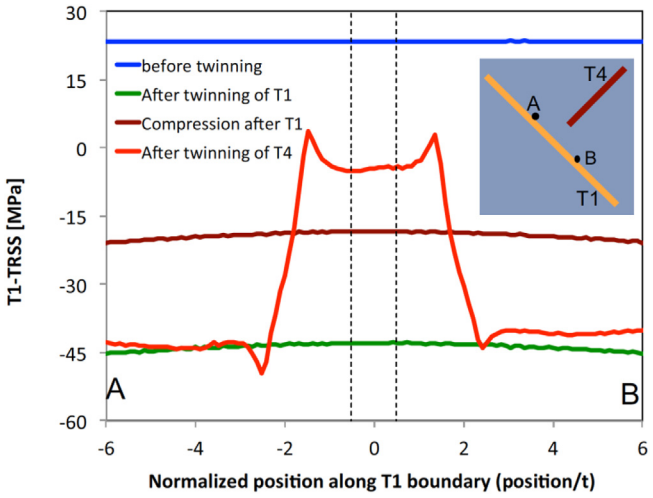

Fig. 3. Twin plane resolved shear stress profile for twin T1 (T1-TRSS) along top interface of T1 from A to B, corresponding to the following simulation steps: before twinning, after twinning of T1, further compression immediately after T1, and after twinning of T4. The spacing s, between T4 tip and T1, is two times the twin thickness t. The position along T1 interface is normalized with respect to twin thickness.

the vicinity of the coherent boundary interface it is negative and tends to arrest twin thickening [27,43,45]. The conditions for forming a twin junction will be determined by the characteristics of the superimposed fields associated with T1 and T4. To determine the driving force for the migration of T1 boundary, the TRSS for the T1 variant along the twin boundary (T1-TRSS) is calculated immediately next to the T1 twin interface on the side closer to T4. Similarly, to determine the driving force for propagating the T4 variant, the TRSS for the T4 variant along the twin boundary (T4-TRSS) is calculated in the matrix region between T1 and T4. First, we discuss the driving force for the migration of the T1 boundary.

To first demonstrate the importance of achieving an equilibrium stress state for the twin-twin configuration, we describe the intermediate stages of stress for one case. In Fig. 3, the T1-TRSS profile along the twin boundary from A to B (see inset) is shown at four stages in the simulation: (1) after imposing initial compression along Y-direction to the twin-free crystal, (2) after introducing twin T1, (3) after further compression along the Y-direction with T1 present to increase the T4-TRSS slightly past the CRSS, and (4) after introducing twin T4 under the final applied strain. As shown in figure insert, the points A and B encompass the junction region. In particular the two vertical dashed lines correspond to the points in the twin boundary where T4 would impinge on T1, i.e., the twin-twin junction points. The final result is a local increase in the T1 driving force, suggesting that prior to contact the boundary of T1 may locally migrate towards T4. As reported in our previous works, the stress concentration developed ahead of the T4 twin tip due to the shear transformation of T4 favors the forward propagation of T4 towards T1. The average T4-TRSS in a small volume in the vicinity of T4 tip is calculated to be 11.24 MPa for $s = 2.0t$. In the remaining calculations only the final relaxed stress state will be presented and analyzed.

Next, we study the variation in driving forces as the two twins draw closer. The EVP-FFT calculations are repeated for different spacings between twin T4 tip and T1, i.e. $s/t = 2.0$, 1.5, 1.0 and 0.5. The driving force for the forward propagation of T4 twin (forward stress at T4 tip) does not vary appreciably with the reduced spacing, and in fact reduces slightly as the twin draws closer. The calculated values are 11.24, 11.22, 11.15 and 11.12 MPa for $s/t = 2.0$, 1.5, 1.0 and 0.5, respectively. Therefore, it appears that the impinging twin is not driven preferentially towards the impinged twin boundary.

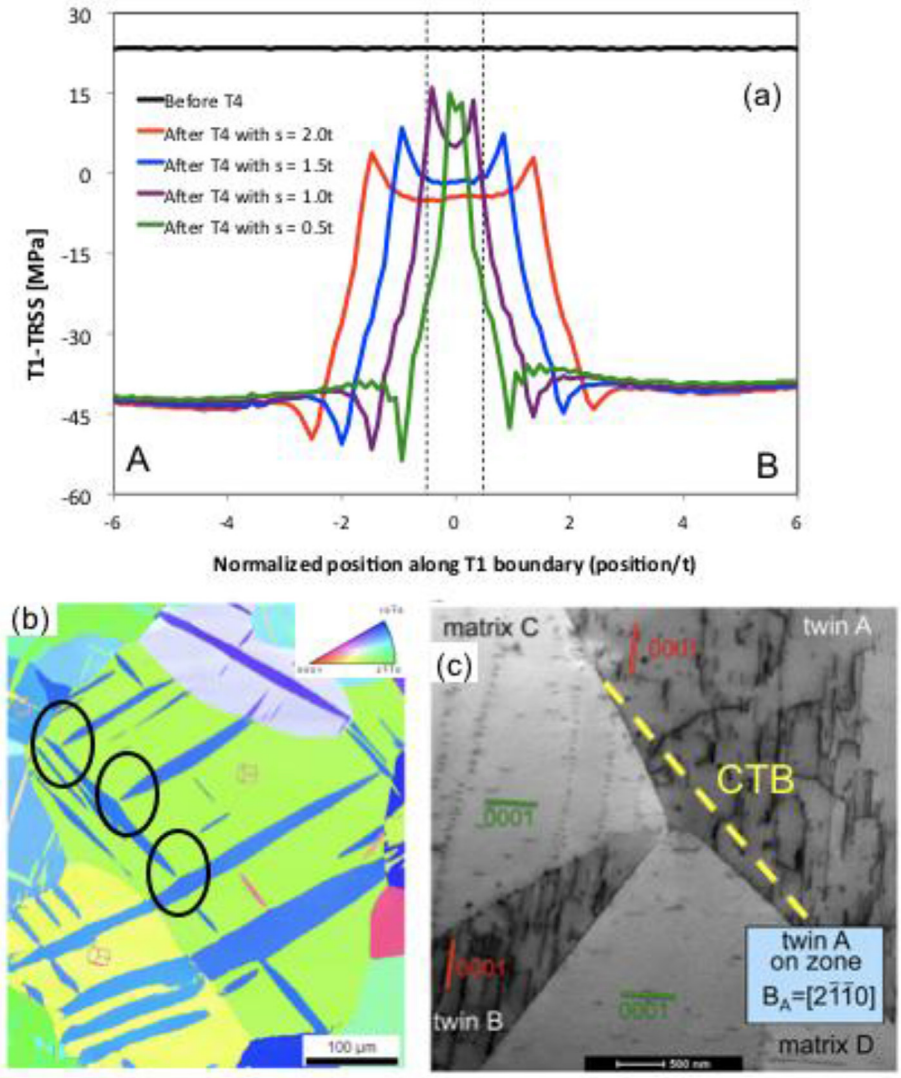

Fig. 4. (a) Twin plane resolved shear stress (T1-TRSS) profile along top interface of T1 for different spacing, $s/t = 2.0$, 1.5, 1.0 and 0.5. (b) EBSD and (c) STEM images showing the large deviation in the twin plane as result of twin-twin interactions. The experimental microscopy images are taken from Morrow et al. [35].

To analyze the concomitant effect on the boundary of T1, we study the TRSS along the T1 boundary as the T4 twin draws closer. Fig. 4(a) shows several T1-TRSS profiles similar to the one in Fig. 3 for different spacings s between the tip of twin T4 and the boundary of T1. Interestingly it shows that the driving force for the local migration of T1 boundary becomes more localized and intense as s/t decreases. This enhancement suggests that the stress state would drive migration of T1 toward T4. Therefore, junction formation is more likely accomplished by boundary migration of the recipient twin (T1) than forward motion of the impinging twin tip (T4).

This perhaps non-intuitive result could explain the twin "reach out" observations recently reported by Morrow et al. (2014), obtained with in-situ TEM and post-mortem EBSD. Fig. 4(b) shows a configuration of $\{10\bar{1}2\}$ tensile twins in an EBSD micrograph of deformed pure Mg where a few 'reach-outs' are marked. Fig. 4(c) shows a scanning transmission electron microscopy (STEM) image of a twin junction shown in Fig. 4(b) clearly displaying the local deviation from the recipient twinning plane at the twin-twin interaction point. These experimental observations provide the evidence for the local migration of the recipient twin from its coherent twin boundary (CTB) to form a twin-twin junction.

3.2. Atomistic simulation of twin-twin junction

Following the EVP-FFT findings, MD simulations are performed to reveal the junction formation process at the atomic scale. Stress field near the junction is shown in Fig. 5. The atoms are colored according to the atomic shear stress τ_{xy}, which is the same as T1-TRSS. We observe that the region at the front of T4 shows greater positive T1-TRSS than the other region along the CTB of T1. Fig. 5(b) shows the variation of T1-TRSS along the two black dashed lines (denoted in Fig. 5(a)) that are 1 nm away from the CTB. The locally high shear stress ahead of T4 will favor the nucleation and glide of twinning dislocations associated with T1. The snapshot in Fig. 5(c) shows that T1 propagates towards T4, growing through the nucleation and gliding of twinning disconnections on the upper and lower CTBs. The preferred nucleation of TDs takes place in the region ahead of the T4 tip, where the shear stress due to T4 is higher. As a result, the upper CTB of T1 migrates towards T4, forming a convex twin boundary. This morphology agrees with experimental observations and is consistent with the configuration of local stresses predicted by the EVP-FFT calculations. Further, we see that the lower twin boundary of T1 migrates downwards through the nucleation and glide of TDs on the lower CTB. Since the local shear stress near the lower CTB is smaller than that near the upper CTB (Fig. 5(b)), less TDs have nucleated on the lower CTB. By the migration of CTBs, T1 grows thicker and the stresses in the model reduce. These simulations confirm the "reach-out" phenomenon suggested by the EVP-FFT calculated local stress states around these two twin lamellae.

A comment is in order concerning the different stress magnitudes predicted by the EVP-FFT and the MD methods. The resolution of the former is on the sub-micron scale, stress values are bounded by plastic slip relaxation, and nanometric details of the twin interface are not captured. The MD calculation, on the other hand, provides local fields at the atomistic scale in the vicinity of interfaces, but no plastic relaxation via dislocations. As a consequence, the stress magnitudes are much larger for MD, as a comparison of Figs. 4a and 5 reveals. From a qualitative perspective, however, the predictions consistent with each other: the field of the T4 twin 'attracts' the T1 twin interface and induces twin-joint formation.

3.3. Twin-twin junction and detwinning

To understand the energetics behind twin-junction formation, the calculated mechanical fields are used to compute the change in the elastic interaction energy in the vicinity of the approaching twin tip as the separation s between the twins decreases. In the simulation, the region R is varied from 0.5 to 1.0 times the thickness of the twin t. Fig. 6 shows that the integrated elastic energy in R decreases as the twins draw closer, indicating that junction formation becomes increasingly favorable. The implication is that the reverse process, detwinning, would be energetically unfavorable once the co-zonal twins form a junction. Accordingly, junction breaking will require an increase in the applied stress under load path reversal or cyclic loading. The junction would "pin" the twins and oppose detwinning, consistent with increased hardening observations reported experimentally [38].

3.4. After twin-twin contact

The studies above show that under a mechanical driving force, the formation of co-zone twin-twin junctions is energetically favorable, provided the load is not reversed. When the applied load is sustained, the twins may continue to accommodate deformation

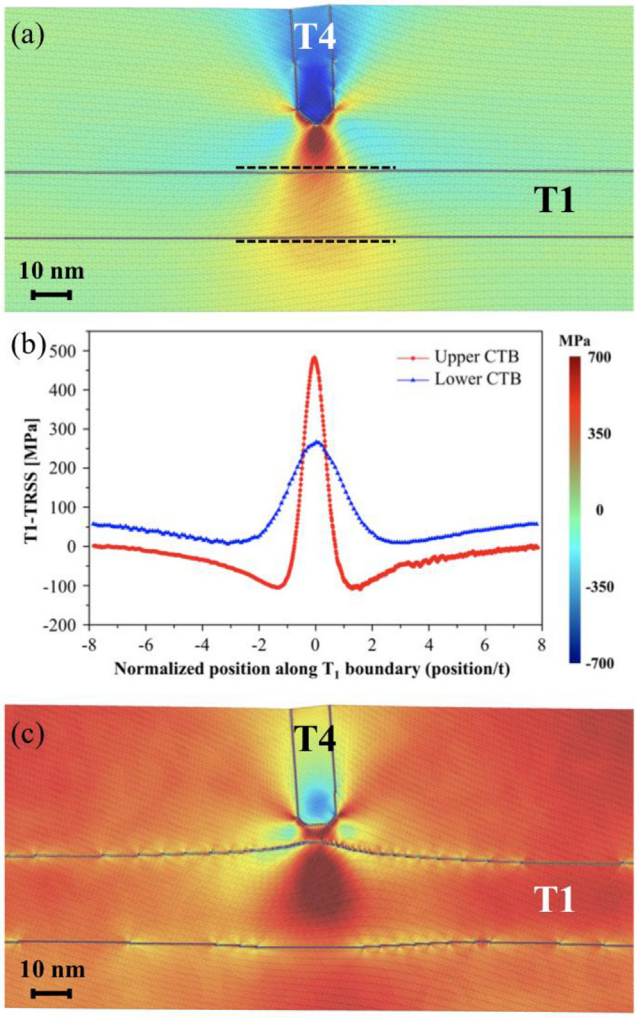

Fig. 5. MD simulations of the (a) unloaded twin-twin interaction. Atoms are colored according to atomic stress τ_{xy} (T1-TRSS). (b) Variation of T1 resolved shear stress (T1-TRSS) on the upper and lower CTBs along the two dashed lines. (c) Formation of twin-twin junction, showing convex twin boundaries associated with preferred nucleation of TDs in the front of T1. Only a portion of the 480 × 120 × 1.6 nm cell used in the MD calculation is shown here.

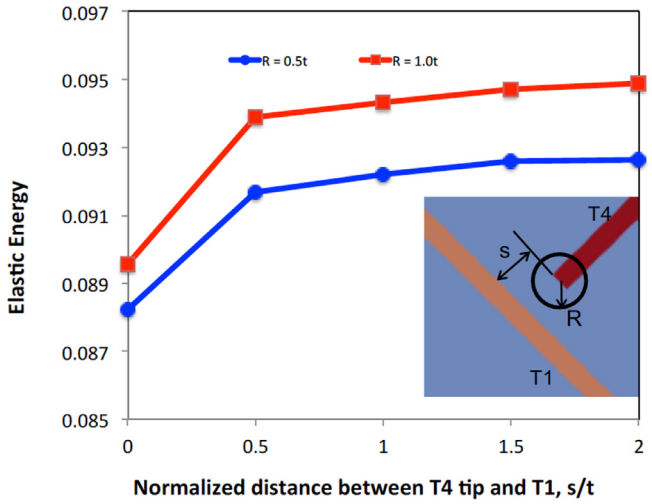

Fig. 6. Average elastic energy in the vicinity of the tip of T4 for different spacings (s/t = 0, 0.5, 1.0, 1.5 and 2.0). The elastic energy is averaged in a small region with radius of R = 0.5t and 1.0t.

by propagating and growing. The question then becomes: how does the twin pair continue to propagate, specifically, does one twin cross the other?

In microscopy of deformed single and polycrystals, twin-twin junctions frequently suggest the existence of an 'apparent crossing' process. In other words, the two twins appear to interpenetrate, wherein the same twin variant of one twin lies on both sides of another twin. Sun et al. [39] speculate, from post-mortem analysis showing one twin partially penetrating another, that crossing is feasible. However, recent evidence from Yu et al. [36], explain the observed configuration as follows: following the formation of the twin-twin junction, both T1 and T4 continue to thicken via emission of twin dislocations, and the final configuration is one of apparent penetration. In addition, Yu et al. [37] show that the stress state and the crystallography of the 'apparent-crossing' domain are unfavorable for twin formation, and that the crystallographic orientation of the domain is not consistent with twin reorientation. Instead, they argue that a new twin of the same variant either nucleates at (and eventually propagates from) the opposite side of the junction, or impinges the opposite side, grows by thickening, and appears like it has been transmitted through the recipient twin.

To understand the process, calculations are carried out to analyze the stress fields associated with the newly formed twin-twin junction. Specifically, we focus on the calculated T4-TRSS fields generated around the twins. This particular component can help us to determine whether the impinging twin would continue to propagate after making contact and, if so, how. Fig. 7(a) shows the T4-TRSS profile along the top interface of T1 (see inset), where

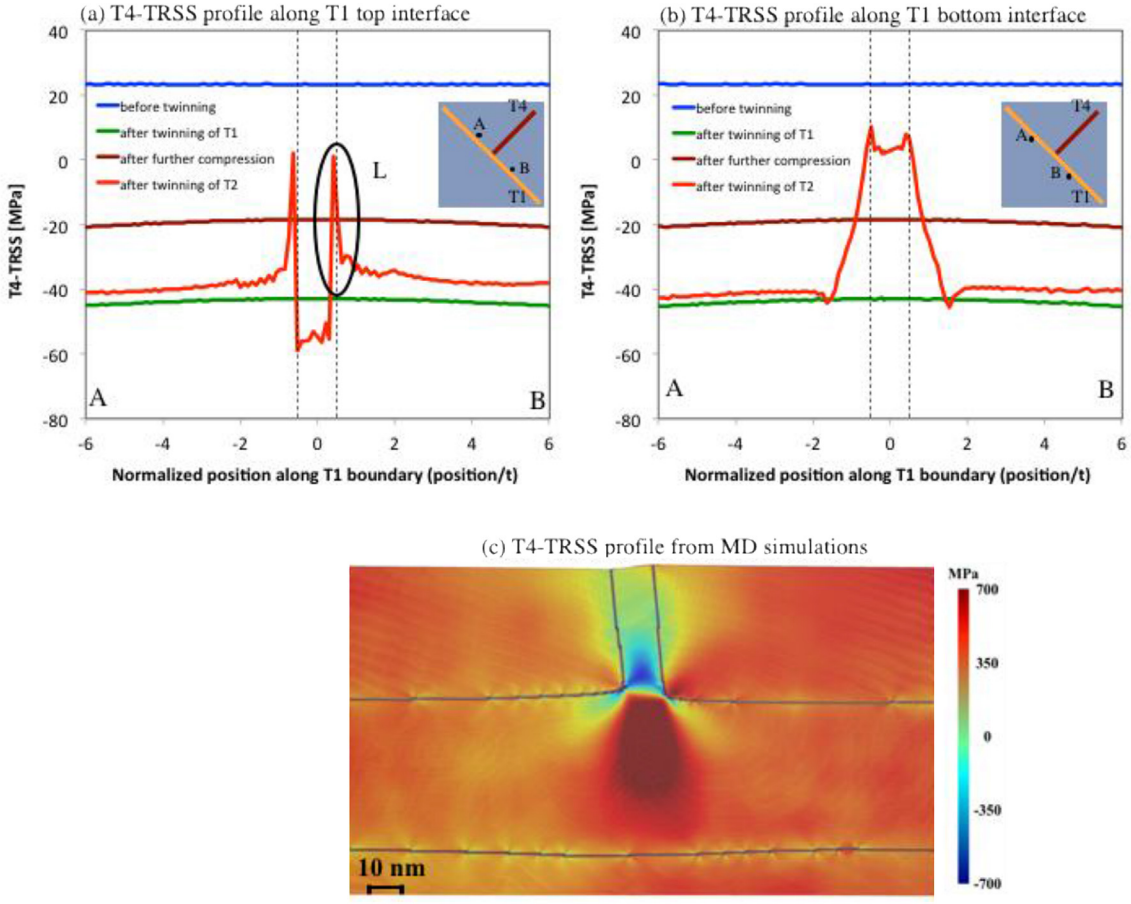

Fig. 7. Twin plane resolved shear stress (TRSS) profile along (a) top and (b) bottom interface of T1 with impinging T4. TRSS profile along top interface prevents the penetration of T4 into T1 and the same TRSS profile along bottom interface suggests that the nucleation of T4 on the opposite side of T1 is possible and may lead to the formation of a 'twin-crossing' configuration. (c) Distribution of T4-TRSS from atomistic simulations after twin junction formation also confirms that the penetration of T4 into T1 is not possible. Only a portion of the 480 × 120 × 1.6 nm cell used in the MD calculation is shown here.

T1 and T4 contact each other. High stress concentrations are observed at the junction at the point marked as L. Provided that T4 twinning dislocations can be supplied to this boundary, the large stress components at the junction can drive twinning dislocations to glide along the T4 boundary, thereby migrating it laterally, and widening the T4 twin after contact. But on the region below the T4 tip inside the T1 boundary, the T4-TRSS is large and negative. There an anti-twinning stress component develops. Such an intense region of anti-twinning TRSS indicates that T4 growth into T1 would not be supported. The matrix region below the opposite facet of T1 experiences a positive T4-TRSS, which suggests that nucleation of the T4 variant is favored, and so T4 propagation from there, leading to a configuration that will appear as a 'crossing' process.

Fig. 7(b) focuses on the T4-TRSS concentration seen along the T1 boundary opposite the contact point (see inset). The T4-TRSS is particularly high along the parts of the boundary where the T4 twin tip meets T1. It is in this region (between the dashed lines) that a new twin is likely to form, of the same type and variant as T4. Formation and extension of a new T4 twin would give the appearance that it has transmitted across the T1 twin. At the same time, nucleation of a twin from the twin boundary is also one of the most likely events [31]. Similar response is also observed from MD simulations and it is shown in Fig. 7(c). Taken together, the results indicate that the approaching twin, upon making contact and forming the junction, would not likely transmit through the existing twin, but instead widen, starting at the junction point, and/or create a new twin of the same variant on the other side of the recipient twin, creating the appearance of a crossed-twin structure.

4. Conclusions

In this work we have employed a full-field crystal plasticity model called Elasto-Visco-Plastic Fast Fourier Transform (EVP-FFT) and atomic-scale molecular dynamics calculations, to understand the role of local stresses on twin-twin junction formation and its characteristics. In developing the micromechanical and atomistic model for the paired twin lamellae interactions within a crystal of Mg, it was important that these simulations were performed in a sequential order, with one twin variant being activated first, followed by the other variant being activated at different relative positions.

The micromechanical simulations are performed for different configurations of stationary twins. The changes in the stress fields and the associated strain energies are calculated for each configuration in the process towards junction formation. The decrease in energy as the twin separation is reduced suggests that under the given loading condition, twin-twin junction formation is energetically favorable. As the dynamic evolution of twins is governed by the motion of interface defects at the atomic scale, it was essential for confirmation to perform molecular dynamics simulations of the process of twin-twin junction formation. Both the atomistic simulations and stress fields from the micromechanics simulations show that the contact of two twins is accomplished by the migration of the impinged twin boundary in the local area of contact, explaining the apparent "reach-out" phenomenon seen in in-situ experiments.

While the results reveal that the formation of a co-zone twin junction in Mg is energetically favorable, they also show, conversely, that retracting of the twins once they are closely interacting, or breaking the twin-twin junction, once formed, are not favorable processes. This result suggests that detwinning of the twin-twin junction upon load reversal or under cyclic loading would be significantly hampered compared to detwinning of single, isolated twins.

Lastly, the model calculations confirm that when one twin impinges on another, it does not directly transmit through the recipient twin. Instead, the local stress state increases in value on the other side of the recipient twin boundary and favors nucleation of a new twin of the same variant as the impinging twin. The result would favor creation of a cross-twinned structure.

The predicted stress concentration due to twin-twin interaction may explain the experimentally observed increase in the flow stress and strain hardening with number of cycles in magnesium [37]. The stress concentration developed as a consequence of twin-twin interaction can locally increase the strength of the material. As a consequence, if the entire single crystal or the grains in the polycrystal develop twin-twin junctions, the global strength of the material will increase. Under cyclic load, the number of twin-twin junctions increases with number of cycles and so it naturally increases the flow stress and strain hardening.

Acknowledgments

This work is fully funded by the U.S. Dept. of Energy, Office of Basic Energy Sciences Project FWP 06SCPE401. M.G. and J.W. were funded through Subcontract LANS RFP No. 364175. MD simulation was completed utilizing the Holland Computing Center of the University of Nebraska, which receives support from the Nebraska Research Initiative. I.J.B. acknowledges financial support from the National Science Foundation, United States (NSF CMMI-1729887).

References

[1] D. Aurbach, Z. Lu, A. Schechter, Y. Gofer, H. Gizbar, R. Turgeman, Y. Cohen, M. Moshkovich, E. Levi, Prototype systems for rechargeable magnesium batteries, Nature 407 (6805) (2000) 724–727.
[2] N.J. Kim, Critical Assessment 6: magnesium sheet alloys: viable alternatives to steels? Mater Sci Tech-Lond 30 (15) (2014) 1925–1928.
[3] M.K. Kulekci, Magnesium and its alloys applications in automotive industry, Int. J. Adv. Manuf. Technol. 39 (9–10) (2008) 851–865.
[4] T.M. Pollock, Weight loss with magnesium alloys, Science 328 (5981) (2010) 986–987.
[5] M.R. Barnett, Twinning and the ductility of magnesium alloys Part I: "Tension" twins, Mat Sci Eng a-Struct 464 (1–2) (2007) 1–7.
[6] M.R. Barnett, Twinning and the ductility of magnesium alloys Part II. "Contraction" twins, Mat Sci Eng a-Struct 464 (1–2) (2007) 8–16.
[7] M.H. Yoo, Slip, twinning, and fracture in hexagonal close-packed metals, Metall Trans A 12 (3) (1981) 409–418.
[8] I.J. Beyerlein, L. Capolungo, P.E. Marshall, R.J. McCabe, C.N. Tome, Statistical analyses of deformation twinning in magnesium (vol 90, pg 2161, 2010), Philos. Mag. A 90 (30) (2010) 4073–4074.
[9] L. Capolungo, P.E. Marshall, R.J. McCabe, I.J. Beyerlein, C.N. Tome, Nucleation and growth of twins in Zr: a statistical study, Acta Mater. 57 (20) (2009) 6047–6056.
[10] P.A. Juan, C. Pradalier, S. Berbenni, R.J. McCabe, C.N. Tome, L. Capolungo, A statistical analysis of the influence of microstructure and twin-twin junctions on twin nucleation and twin growth in Zr, Acta Mater. 95 (2015) 399–410.
[11] A. Khosravani, D.T. Fullwood, B.L. Adams, T.M. Rampton, M.P. Miles, R.K. Mishra, Nucleation and propagation of {1 0(1)over-bar2} twins in AZ31 magnesium alloy, Acta Mater. 100 (2015) 202–214.
[12] M.A. Kumar, M. Wroński, R.J. McCabe, L. Capolungo, K. Wierzbanowski, C.N. Tomé, Role of microstructure on twin nucleation and growth in HCP titanium: a statistical study, Acta Mater. 148 (2018) 123–132.
[13] G. Proust, C.N. Tome, A. Jain, S.R. Agnew, Modeling the effect of twinning and detwinning during strain-path changes of magnesium alloy AZ31, Int. J. Plast. 25 (5) (2009) 861–880.
[14] M.A. Kumar, I.J. Beyerlein, R.A. Lebensohn, C.N. Tome, Modeling the effect of alloying elements in magnesium on deformation twin characteristics, Mineral Met Mat Ser (2017) 159–165.
[15] M.A. Kumar, I.J. Beyerlein, C.N. Tome, A measure of plastic anisotropy for hexagonal close packed metals: application to alloying effects on the formability of Mg, J. Alloy. Comp. 695 (2017) 1488–1497.
[16] M. Lentz, M. Risse, N. Schaefer, W. Reimers, I.J. Beyerlein, Strength and ductility with {10(1)over-bar1} - {10(1)over-bar2} double twinning in a magnesium alloy, Nat. Commun. 7 (2016).
[17] Q. Ma, B. Li, E. Marin, S. Horstemeyer, Twinning-induced dynamic recrystallization in a magnesium alloy extruded at 450 C, Scripta Mater. 65 (9) (2011) 823–826.
[18] B.A. Simkin, B.C. Ng, M.A. Crimp, T.R. Bieler, Crack opening due to deformation twin shear at grain boundaries in near-gamma TiAl, Intermetallics 15 (1)

(2007) 55–60.
[19] D. Xu, E. Han, Relationship between fatigue crack initiation and activated {101 2} twins in as-extruded pure magnesium, Scripta Mater. 69 (9) (2013) 702–705.
[20] Q. Yu, Y. Jiang, J. Wang, Cyclic deformation and fatigue damage in single-crystal magnesium under fully reversed strain-controlled tension–compression in the [100] direction, Scripta Mater. 96 (2015) 41–44.
[21] Q. Yu, J. Zhang, Y. Jiang, Fatigue damage development in pure polycrystalline magnesium under cyclic tension–compression loading, Mater. Sci. Eng., A 528 (25–26) (2011) 7816–7826.
[22] M.R. Barnett, Z. Keshavarz, A.G. Beer, D. Atwell, Influence of grain size on the compressive deformation of wrought Mg-3Al-1Zn, Acta Mater. 52 (17) (2004) 5093–5103.
[23] T. Bieler, L. Wang, A. Beaudoin, P. Kenesei, U. Lienert, In situ characterization of twin nucleation in pure Ti using 3D-XRD, Metall. Mater. Trans. 45A (1) (2014) 109–122.
[24] C.F. Guo, R.L. Xin, C.H. Ding, B. Song, Q. Liu, Understanding of variant selection and twin patterns in compressed Mg alloy sheets via combined analysis of Schmid factor and strain compatibility factor, Mat Sci Eng a-Struct 609 (2014) 92–101.
[25] M.A. Kumar, I.J. Beyerlein, R.J. McCabe, C.N. Tome, Grain neighbour effects on twin transmission in hexagonal close-packed materials, Nat. Commun. 7 (2016), 13826.
[26] M.A. Kumar, I.J. Beyerlein, C.N. Tome, Grain size constraints on twin expansion in hexagonal close packed crystals, J. Appl. Phys. 120 (15) (2016).
[27] M.A. Kumar, I.J. Beyerlein, C.N. Tome, Effect of local stress fields on twin characteristics in HCP metals, Acta Mater. 116 (2016) 143–154.
[28] Z.Z. Shi, Y.D. Zhang, F. Wagner, T. Richeton, P.A. Juan, J.S. Lecomte, L. Capolungo, S. Berbenni, Sequential double extension twinning in a magnesium alloy: combined statistical and micromechanical analyses, Acta Mater. 96 (2015) 333–343.
[29] R. Xin, C. Guo, Z. Xu, G. Liu, X. Huang, Q. Liu, Characteristics of long {10-12} twin bands in sheet rolling of a magnesium alloy, Scripta Mater. 74 (2014) 96–99.
[30] M. Arul Kumar, B. Leu, P. Rottmann, I.J. Beyerlein, Characterization of Staggered Twin Formation in HCP Magnesium, Springer International Publishing, Cham, 2019, pp. 207–213.
[31] H. El Kadiri, J. Kapil, A.L. Oppedal, L.G. Hector, S.R. Agnew, M. Cherkaoui, S.C. Vogel, The effect of twin-twin interactions on the nucleation and propagation of {10(1)over-bar2} twinning in magnesium, Acta Mater. 61 (10) (2013) 3549–3563.
[32] M.Y. Gong, J.P. Hirth, Y. Liu, Y. Shen, J. Wang, Interface structures and twinning mechanisms of {(1)over-bar012} twins in hexagonal metals, Mater Res Lett 5 (7) (2017) 449–464.
[33] M.Y. Gong, S. Xu, Y. Jiang, Y. Liu, J. Wang, Structural characteristics of {1 012} non-cozone twin-twin interactions in magnesium, Acta Mater. 159 (2018) 65–76.
[34] M. Lentz, R.S. Coelho, B. Camin, C. Fahrenson, N. Schaefer, S. Selve, T. Link, I.J. Beyerlein, W. Reimers, In-situ, ex-situ EBSD and (HR-)TEM analyses of primary, secondary and tertiary twin development in an Mg-4 wt%Li alloy, Mat Sci Eng a-Struct 610 (2014) 54–64.
[35] B.M. Morrow, E.K. Cerreta, R.J. McCabe, C.N. Tome, Toward understanding twin-twin interactions in hcp metals: utilizing multiscale techniques to characterize deformation mechanisms in magnesium, Mat Sci Eng a-Struct 613 (2014) 365–371.
[36] Y. Pei, A. Godfrey, J. Jiang, Y.B. Zhang, W. Liu, Q. Liu, Extension twin variant selection during uniaxial compression of a magnesium alloy, Mat Sci Eng a-Struct 550 (2012) 138–145.
[37] Q. Yu, J. Wang, Y.Y. Jiang, R.J. McCabe, N. Li, C.N. Tome, Twin-twin interactions in magnesium, Acta Mater. 77 (2014) 28–42.
[38] Q. Yu, J. Wang, Y.Y. Jiang, R.J. McCabe, C.N. Tome, Co-zone {(1)over-bar012} twin interaction in magnesium single crystal, Mater Res Lett 2 (2) (2014) 82–88.
[39] S. Xu, L.S. Toth, C. Schuman, J.S. Lecomte, M.R. Barnett, Dislocation mediated variant selection for secondary twinning in compression of pure titanium, Acta Mater. 124 (2017) 59–70.
[40] Q. Sun, X. Zhang, Y. Ren, L. Tan, J. Tu, Observations on the intersection between 1012 twin variants sharing the same zone axis in deformed magnesium alloy, Mater. Char. 109 (2015) 160–163.
[41] L. Jiang, J.J. Jonas, Effect of twinning on the flow behavior during strain path reversals in two Mg (+ Al, Zn, Mn) alloys, Scripta Mater. 58 (10) (2008) 803–806.
[42] L. Jiang, J.J. Jonas, A.A. Luo, A.K. Sachdev, S. Godet, Influence of {10-12} extension twinning on the flow behavior of AZ31 Mg alloy, Mater. Sci. Eng., A 445 (2007) 302–309.
[43] M.A. Kumar, I.J. Beyerlein, R.A. Lebensohn, C.N. Tome, Modeling the effect of neighboring grains on twin growth in HCP polycrystals, Model Simul. Mater. Sc 25 (6) (2017), 064007.
[44] M.A. Kumar, I.J. Beyerlein, R.A. Lebensohn, C.N. Tome, Role of alloying elements on twin growth and twin transmission in magnesium alloys, Mat Sci Eng a-Struct 706 (2017) 295–303.
[45] M.A. Kumar, A.K. Kanjarla, S.R. Niezgoda, R.A. Lebensohn, C.N. Tome, Numerical study of the stress state of a deformation twin in magnesium, Acta Mater. 84 (2015) 349–358.
[46] M.A. Kumar, B. Clausen, L. Capolungo, R.J. McCabe, W. Liu, J.Z. Tischler, C.N. Tome, Deformation twinning and grain partitioning in a hexagonal close-packed magnesium alloy, Nat. Commun. 9 (2018) 4761.
[47] J. Michel, H. Moulinec, P. Suquet, A computational method based on augmented Lagrangians and fast Fourier Transforms for composites with high contrast, Cmes-Comp. Model. Eng. Sci. 1 (2) (2000) 79–88.
[48] H. Moulinec, P. Suquet, A fast numerical method for computing the linear and nonlinear mechanical properties of composites, Comp. Rendus De L Academie Des Sciences Serie Ii 318 (11) (1994) 1417–1423.
[49] R.A. Lebensohn, N-site modeling of a 3D viscoplastic polycrystal using Fast Fourier Transform, Acta Mater. 49 (14) (2001) 2723–2737.
[50] R. Brenner, R.A. Lebensohn, O. Castelnau, Elastic anisotropy and yield surface estimates of polycrystals, Int. J. Solids Struct. 46 (16) (2009) 3018–3026.
[51] R.A. Lebensohn, R. Brenner, O. Castelnau, A.D. Rollett, Orientation image-based micromechanical modelling of subgrain texture evolution in polycrystalline copper, Acta Mater. 56 (15) (2008) 3914–3926.
[52] R.A. Lebensohn, M.I. Idiart, P.P. Castaneda, P.G. Vincent, Dilatational viscoplasticity of polycrystalline solids with intergranular cavities, Philos. Mag. A 91 (22) (2011) 3038–3067.
[53] A.K. Kanjarla, R.A. Lebensohn, L. Balogh, C.N. Tome, Study of internal lattice strain distributions in stainless steel using a full-field elasto-viscoplastic formulation based on fast Fourier transforms, Acta Mater. 60 (6–7) (2012) 3094–3106.
[54] R.A. Lebensohn, A.K. Kanjarla, P. Eisenlohr, An elasto-viscoplastic formulation based on fast Fourier transforms for the prediction of micromechanical fields in polycrystalline materials, Int. J. Plast. 32–33 (2012) 59–69.
[55] P. Eisenlohr, M. Diehl, R.A. Lebensohn, F. Roters, A spectral method solution to crystal elasto-viscoplasticity at finite strains, Int. J. Plast. 46 (2013) 37–53.
[56] I.J. Beyerlein, R.J. McCabe, C.N. Tome, Effect of microstructure on the nucleation of deformation twins in polycrystalline high-purity magnesium: a multi-scale modeling study, J. Mech. Phys. Solid. 59 (5) (2011) 988–1003.
[57] R.F.S. Hearmon, The elastic constants of anisotropic materials, Rev. Mod. Phys. 18 (3) (1946) 409–440.
[58] G. Simmons, H. Wang, Single Crystal Elastic Constants and Calculated Aggregate Properties: A Handbook, MIT press, 1971.
[59] X.Y. Liu, J.B. Adams, F. Ercolessi, J.A. Moriarty, EAM potential for magnesium from quantum mechanical forces, Model Simul. Mater. Sc 4 (3) (1996) 293–303.
[60] J. Wang, J.P. Hirth, C.N. Tome, ((1)over-bar0 1 2) Twinning nucleation mechanisms in hexagonal-close-packed crystals, Acta Mater. 57 (18) (2009) 5521–5530.
[61] J. Wang, L. Liu, C.N. Tome, S.X. Mao, S.K. Gong, Twinning and De-twinning via glide and climb of twinning dislocations along serrated coherent twin boundaries in hexagonal-close-packed metals, Mater Res Lett 1 (2) (2013) 81–88.
[62] D.M. Barnett, J. Lothe, Image force theorem for dislocations in anisotropic bicrystals, J. Phys. F Met. Phys. 4 (10) (1974) 1618–1635.
[63] J.W. Christian, S. Mahajan, Deformation twinning, Prog. Mater. Sci. 39 (1–2) (1995) 1–157.
[64] A. Ostapovets, A. Serra, Characterization of the matrix-twin interface of a (10(1)over-bar2) twin during growth, Philos. Mag. A 94 (25) (2014) 2827–2839.